Design and Prototype of a Microgrid for Enhancing Reliability of Power Supply for Artificial Intelligence Data Centers

RAMON ZINTZUN, ETHAN HOANG, JARED WONG, AKANKSHA KATTA,
VINH NGUYEN, ALEX VILLANEDA, GERARDO MAXIMO, HA THU LE*
Department of Electrical and Computer Engineering,
California State Polytechnic University, Pomona,
Pomona, California 91768,
UNITED STATES OF AMERICA

Corresponding Author

Abstract: - Along with increasing use of artificial intelligence (AI), power supply for AI data centers has become critical for ensuring their continuous operation to provide multitude of services. AI data centers rely heavily on utility grids for their high power demand. However, it is known that utility grids are vulnerable to weather and other conditions which lead to outages. Hence, we design a microgrid that makes use of solar PV and battery technologies to increase reliability of power supply for AI data centers. It also reduces their carbon footprint and power demand from the utility grids. A real-world 5.85-MW AI data center in Wyoming state is used as a case study. The microgrid is designed to provide 60% of the center power demand from solar PV and 40% from utility. Additionally, it has a battery storage system capable of providing power for up to 18.2 hours. The battery is charged during high solar production hours and supplies critical loads in the data center at night. A prototype of the microgrid is built for evaluating the design concepts and the system performance. The testing results show that the prototype works properly. It supplies critical and non-critical loads in an automated manner using a microcontroller. For example, at battery state of charge (SOC) of 90% all the loads are operational. At the battery SOC of 40%, the microcontroller automatically turns off non-critical loads while keeping critical loads. The microgrid increases reliability of power supply to data centers because it has battery back-up power. The solar PV system adds to the microgrid reliability because it can supply power to data centers under utility outage conditions. The microgrid design is applicable to all data centers where space and resource are available for solar PV. The microgrid enhances AI data center reliable operation while reducing power demand stress on utility grids.

Key-Words: - Artificial intelligence (AI), battery, converter, data center, inverter, microgrid, microcontroller, solar PV.

Received: May 24, 2025. Revised: January 9, 2026. Accepted: May 7, 2026. Published: July 9, 2026.

1 Introduction

Microgrids represent the future smart grid infrastructures and have undergone significant research in recent years, particularly concerning critical infrastructure such as AI data centers. Microgrid systems have progressed from basic backup systems to energy management systems that can integrate various energy sources through electrical framework and advanced control methods, [1]. The transformation towards microgrid systems has been driven by the growing need for sustainable power solutions, [2].

The incorporation of renewable generating sources into microgrids has become more important for AI data centers seeking to improve security while retaining reliability, [3]. Traditionally, data center's power supply has relied on conventional utility power supply backed by back-up generators, [4].

However, recent research has shown that the traditional approach can be improved by using renewable energy sources and novel energy storage solutions, [5], [6]. A thorough study of utility data indicates that, while beneficial hybrid microgrids powered by local electricity generation had certain limits [5]. Studies on data center utility models show that such facilities can benefit from demand response strategies in addition to local electricity generation, particularly during peak demand hours, [6], [7]. Further, off-grid renewable energy generation in data centers can be successfully adopted with proper evaluation and management processes, [7], [8].

Advancement of information and communication technology has enabled sophisticated management strategies and better integration of energy sources, [8]. Recent developments in microgrid technology have led to a substantial enhancement in reliability and efficiency by employing hybrid systems, [9]. This improvement is supported by extensive research on data center integration and its interaction with local generation, energy storage and the power grid, [10].

Detailed economic analysis of the deployment of battery storage in the data center microgrids has been shown to have significant improvements in cost savings, emission reduction, and reliability, [11]. The incorporation of energy storage devices has emerged as a crucial factor for data center's operation efficiency, especially when energy storage devices are integrated with renewable energy sources, [12].

Past studies have established several significant approaches to data center power management. They include developing renewable energy integration systems utilizing standard unidirectional power flow, [7], implementing basic energy storage systems with a major emphasis on capacity optimization, [12], and applying traditional renewable energy integration methodologies with small grid-tied systems, [1]. While these studies demonstrated the potential for renewable energy in data centers, they employed traditional power conversion technologies, limiting operational flexibility.

These present implementations, while effective, have certain limitations. Vargas et al., [5], uses traditional DC-AC conversion systems, which require several power conversion stages, limiting total system efficiency. Karimian et al., [8], adopted standard control systems that lack the ability for rapid transitions between power sources. These techniques, while important, do not solve the need for seamless power flow management across numerous sources while preserving optimal power quality. Microgrids with solar PV and battery have been considered for multiple applications and have shown promising effectiveness, [13], [14], [15], [16].

Our project expands upon prior implementations by designing a solar microgrid system with bidirectional DC-DC converter. This approach eliminates the requirement for multiple power conversion stages, increasing system efficiency as well as providing a continuous power supply during source transitions. The architecture allows for direct solar charging of the batteries at peak production and easy transition between power sources. A real-world 5.85-MW data center is used as a case study. Using distributed integrated control architectures, [17], and contemporary data center networking, [18], the microgrid is designed to supply 60% of center power demand while the remaining 40% is provided by the utility grid.

The study focuses on three main objectives:

1) Design an hybrid renewable energy system for enhancing data center power supply reliability and service continuity while supporting environmental sustainability.
2) Design an automated energy management system for supplying critical and non-critical loads appropriately.
3) Evaluate the effectiveness of using solar PV and battery in enhancing reliability of power supply for data centers.

2 Theoretical Design of Microgrid and Parameters

The microgrid design uses a data center located in Cheyenne, Wyoming state, USA, which has a peak power demand of 5.85 MW. Its total crticial load is around 5.35 MW, as shown in Table 1. The proposed microgrid combines several power sources and conversion pathways as shown on Figure 1 and Figure 2. The Cheyenne site can support a large solar PV system given regional solar irradiance levels and lots of land available around the data center location. A 5.85-MW facility may be considered small-to-medium size for AI data centers as modern data center size can be much bigger. Though, the 5.85-MW facility can still serve as a good case to investigate the concept of using solar PV and battery to improve its power sypply reliability.

From Figure 2, the solar PV system connects through circuit breakers that serve as a safety device for the protection of the installation. The breakers are heavy-duty and built to withstand the high voltage DC applications. DC circuit breakers are commercially available with voltage rating from 12V to 1500V DC and current rating based on requirements for solar installations. DC circuit breakers are constructed to both manage the requirements for direct current switching and neutralize the arc during outage conditions, which is important for renewable energy systems. The utility grid connection (Figure 1) is intended to supply 40% of the center power demand, where the loads to be supplied include mostly noncritical and some critical.

The system's automatic transfer switch (Figure 2) is used to select utility grid power and solar-battery power appropriately. It is intended to prioritize renewable energy whenever feasible and only use the grid power when absolutely required. This setup enables the control system to effectively manage power distribution by juggling load demands, battery charging, and solar power generation at the same time.

From Figure 2, there are two ways of power conversion in the microgrid. One is DC-AC where an inverter is used to convert DC power into AC to supply AC loads. The other is DC-DC where a converter is used to convert DC power of one voltage to DC power of different voltage to supply different DC loads. In this setup, the battery system and solar panels produce DC power, which the inverter transforms into AC to power AC vital equipment. The second method employs the use of a Buck-Boost converter to deliver the suitable DC power to server racks and other DC equipment. Circuit breakers are installed on both sides of the conversion path for protection.

2.1 Data Center Power Consumption Analysis

The microgrid is designed to cater to 60% of the center total power demand while 40% is provided by the utility grid. The reason to rely on the utility grid for 40% of power demand is to lower the size and cost of the solar system. The total peak load on the facility is 5.85 MW. The calculated daily energy consumption at 60% proportion (i.e., the demand to be covered by the microgrid solar and battery systems) is 76427 kWh, where daytime energy consumption is 44253 kWh (07:15am–06:00pm, around 11 hours) and nighttime energy consumption is 32173 kWh (12:00am–07:00am and 06:00pm–11:45pm, around 13 hours). The center's daily energy consumption is calculated using its 24-hour load curve on Figure 3.

The data center load curve of Figure 3 is generated using 96 power values in a day at 15-minute intervals. The values are determined by normalizing the California data center load curve on Figure 4 (i.e., converting it to percentage by dividing by its peak load), [9], and multiplying the normalized curve by the center peak load of 5.85MW. The curve gives a complete picture of the data center load profile and energy consumption for 24- hour day.

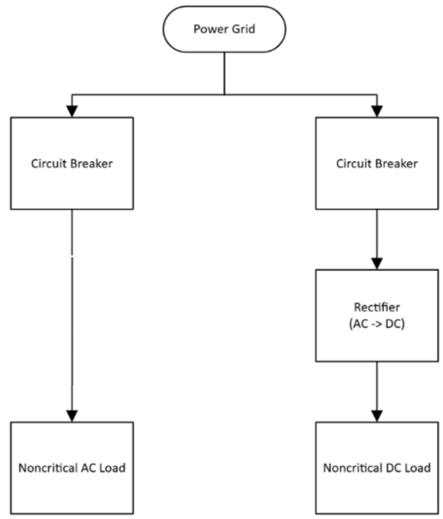

Fig. 1: Utility grid connection for the data center
Source: created by the authors.

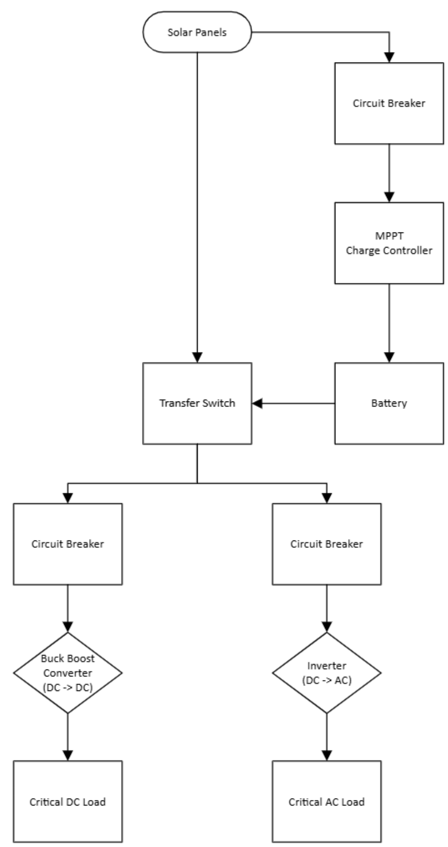

Fig. 2: Microgrid connection that shows power supply from solar PV and battery to critical loads
Source: created by the authors.

Table 1. Data center power consumption by critical loads

Component	Power usage (MW)
Cooling	0.8845
Server	3.5830
Lighting	0.1542
Battery charging	0.5653
Surveillance and Computers	0.1650
Total	**5.352**

Source: created by the authors.

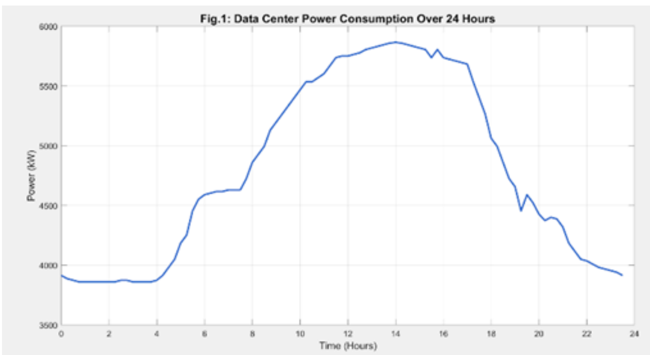

Fig. 3: Data center 24-hour power profile
Source: created by the authors.

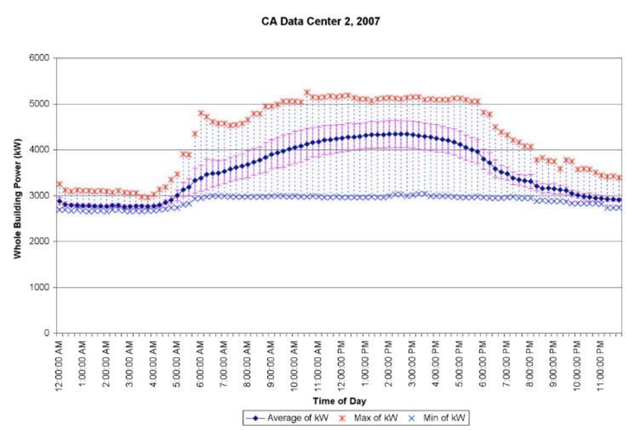

Fig. 4: California data center 24-hour power consumption profile
Source: [19].

2.2 Solar PV System Size and Energy Production

The solar PV system provides power to the load during the daytime and charge the battery for night operation. According to the results shown by the center daily load data, 44253 kWh needs to be provided by daytime and 32173 kWh needs to be provided during nighttime using the battery. Assuming energy conversion loss of 5% due to solar energy DC-AC conversion for serving AC loads and 10% due to battery charging-discharging process, the solar PV system must provide 44253x1.05= 46466 kWh for daytime load demand and 32173x1.1=35391 kWh for nighttime load demand. It follows that the total energy that the solar PV system must provide is 46466+35391=81857 kWh per day (i.e., 24-hour period). Note that only part of the 44253 kWh solar energy is converted to AC for supplying AC loads during daytime. Hence, the above 5-percent loss being applied to 44253 kWh is a conservative approach.

The solar PV system power rating is determined using the U.S. National Renewable Energy Laboratory (NREL) PVWatts calculator, [20]. PVWatts is a web-based calculator that estimates the energy production of solar PV systems for specific locations worldwide using solar resource data and other system parameters. The solar system is located in Cheyenne, Wyoming, USA, which is assumed to use standard modules and 2-axis tracking where the system loss (due to shading, soiling, wiring, etc.) is 14.08%. The solar PV system estimated size is 13600kW which produces 82367 kWh per day on average (30064032 kWh per year). Its daily average energy production satisfies the required solar energy calculated above (81857 kWh per day). The annual average solar radiation for the location is 7.76 kWh/m2/day.

Notably, Wyoming state has a Net Metering program where solar PV system owners can output surplus energy into the utility grids for compensation. Hence, the surplus energy from the solar system (511kWh/day x 365 days = 186400 kWh per year) may be sold back to the host utility (Black Hills Energy) for compensation. If this surplus energy is used to supply the data center loads, the microgrid would provide more than 60% of the center energy demand.

Comparing typical daily solar generation curves with the data center 24-hour power profile on Figure 3 suggests that solar high generation duration matches the peak demand of the data center during daytime hours (e.g., 10am-4pm). This is an advantage of using the solar PV system to supply the data center.

2.3 Sizing of Battery Energy Storage System (BESS)

The battery system's size is determined based on the data center nighttime energy need of 35391 kWh per day (including battery 10% charge-discharge efficiency). The center's peak load during nighttime, estimated using Figure 3, is around 4625 kW. Assume that the battery supports 60% of the center peak load at night, the power rating of the battery should be 4625x0.6=2775kW. In addition, assume that Li-ion cells are used in the battery system where the battery depth of discharge is 30% (i.e., the battery can discharge up to 70% of its energy capacity), the battery energy capacity should be 35391/0.7=50558 kWh. It follows that the battery duration is 50558 kWh/2775kW = 18.2 hours (fully discharged) while the effective duration is 35391kWh/2775kW=12.8 hours (discharging 70% of its energy capacity). Notably, if less conservative depth of discharge is used, namely 80%-90%, which is acceptable for LiFePO4 batteries, the battery size will be smaller.

2.4 Inverter Size

From Figure 2, the inverter is used to convert part of solar PV system DC power or battery power to AC to supply the data center AC loads. The center total AC load is estimated to be 15367 kW. The inverter rating is selected to be 120% of the total AC load, or 18440 kW. This is a conservative rating to accommodate power loss during the power inverting process and allow some expansion room in case the center AC load demand increases.

3 Prototype Design and Parameters

For evaluating the microgrid design concepts and its performance, a prototype is built by scaling down the theoretical microgrid. The prototype resembles the microgrid in most aspects, such as having a solar PV panel and battery as power sources, and AC and DC loads. The prototype block diagram is shown on Figure 5 while the electrical diagram is shown on Figure 6.

From Figure 5, the solar panel is the primary source for the scaled-down microgrid. It is connected to an MPPT (Maximum Power Point Tracking) Charge Controller, which optimizes energy harvest and manages battery charging. The battery stores energy for use when solar generation is insufficient or not available. The power conversion is managed through two primary converters: an inverter to AC load (represented by an AC fan), and a Buck Converter to DC loads (represented by a DC fan, LED strips, and resistors; resistors are not shown on Figure 5). The power distribution is automatically managed by a microcontroller and relays. The control scheme distributes power to loads based on power availability and prioritizes critical loads over non-critical.

For scaling down the realistic microgrid design to the small prototype, the battery system is reduced to a commercial LiFePO4 12.8V 50Ah battery, and the solar PV system in the theoretical design is represented by a 255-W solar panel. A buck converter is used for DC voltage regulation and a small inverter is used for powering AC loads. The prototype components resemble the microgrid sub-systems and functions. The resemblance of the prototype with the microgrid supports evaluation of the microgrid design concepts and performance.

4 Prototype Implementation and Evaluation

4.1 Implementation of Prototype

Table 2 lists the scaled-down system main components and costs, [21], [22], [23], [24], [25]. It includes a solar panel, [21], that convert the sunlight into 255 watts of DC power at 30.8 volts. The generated electricity is then supplied to the inverter, [22], which converts the DC power to 110V AC for usage by the AC load.

As described previously for Figure 5, a LiFePO4 12.8V, 50Ah battery, [23], is used to store energy for use when necessary. This resembles the microgrid operation where the battery system stores solar energy during the day then supplies the data center loads at nighttime and during low solar power production periods. The charge controller, [24], regulates the battery charging process. It keeps the battery from overcharging to preserve its longevity. Furthermore, a buck converter, [25], is included to regulate the DC power. Its input voltage range is 6VDC-32VDC and output voltage range is 1.5VDC-32VDC. The buck converter lowers the input voltage to supply the prototype DC loads.

The prototype electrical diagram of Figure 6 shows how components connect with each other. The loads to be connected are not shown. An arrangement of indication of LEDs at different regions marks the operational status of this system. The circuits are switchable into individual modules so that they may be energized by manual control. While the DC-DC converter and the DC-AC inverter perform power transformation, it is the busbars that convey electric power to different parts of the system. Resistors, inductors, and capacitors comprise the devices used for limiting and filtering current so that clean power is delivered to the loads.

The prototype power distribution is managed automatically by the microcontroller according to the control logic shown on Figure 8. The power availability in the battery is determined by sensing the battery voltage and using its SOC curve shown on Figure 7 and Table 3 in Appendix.

Pseudocode of microcontroller:

- START.
- Sensors read how many watts are needed in total to power all loads in the prototype.
- Next, it reads the power being generated by the solar PV panel along with the power being discharged by the battery.
- If the PV source is greater than the load demand, the system checks the state of charge of the battery.
- If the battery is not fully charged, connect the battery and charge it until it is fully charged.
- When the battery is fully charged, we can isolate it and check if the PV power produced is still greater than the load demand.
- If so, the system enters an idle position where it does not charge the battery and continues using the PV source to power all loads until the load demand is more than the PV source.
- If the PV source power production is less than the amount of the load being demanded, we check the SOC of the battery and if it is more than 30%, we connect the battery to the system and allow it to discharge and supply the difference in power that the PV source is not able to provide.
- If the battery state of charge is less than 30%, we disconnect the non-critical loads and isolate the battery to charge it.

4.2 Evaluation of Prototype Performance

The prototype was tested using a voltage controller to simulate different states of charge of the battery. This was done to ensure that the relays were working the way they were programmed by keeping critical power on as long as possible while protecting the battery. The completed prototype is shown on Figure 9. The most important outcomes are provided on Figure 10, Figure 11, Figure 12.

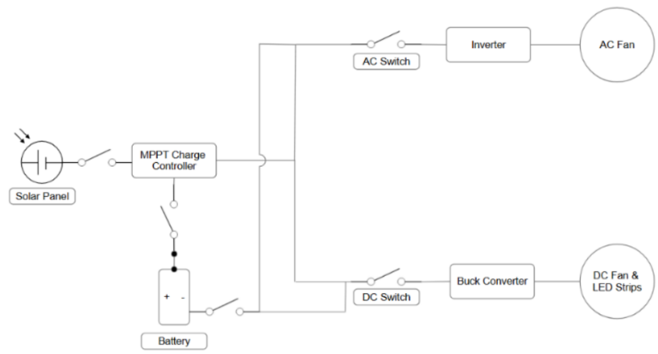

Fig. 5: Prototype block diagram; the DC loads connected to the Buck Converter include resistors (not shown on the figure)
Source: created by the authors.

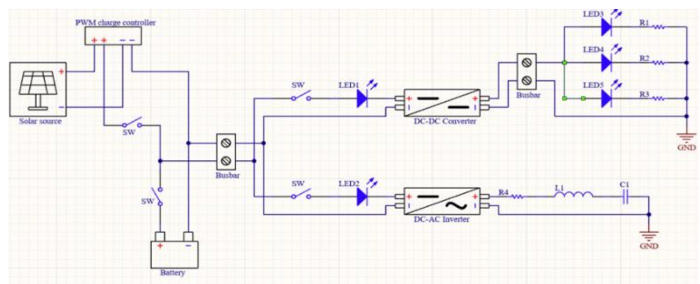

Fig. 6: Prototype electrical diagram; the loads to be connected are not shown
Source: created by the authors.

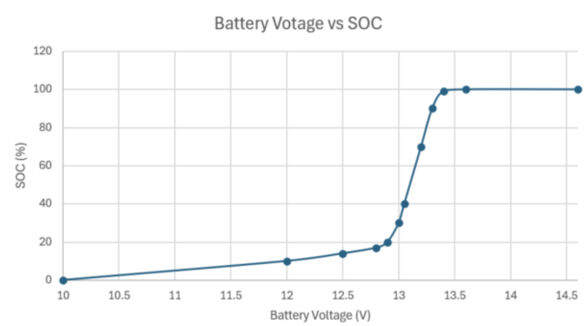

Fig. 7: Battery voltage versus state of charge (SOC)
Source: [26]

In Figure 10, we evaluate the microgrid physical model being powered down. No power is supplied to both AC and DC loads because the battery SOC is below 30%. The relay LEDs are all on, indicating no power is being supplied to the AC and DC loads. When the battery voltage is below 12.9V, the system enters a protective shutdown mode where all relays are effectively turned off to prevent further battery discharge. In this state, the relay control pins RELAY_CHARGING, RELAY_DC_CRIT_AC and

RELAY_DC_NONCRIT are set to LOW. Since our relay modules use inverted logic, a LOW signal actually activates the relay, meaning current is cut off to the connected loads. As a visual indicator, all red LEDs on the relay board are turned on, signaling that the relays are actively shutting off power. This is a safety mechanism designed to preserve battery life during low voltage conditions. The system remains in this mode until the battery voltage rises back above 12.9V (i.e., the battery SOC is over 30%).

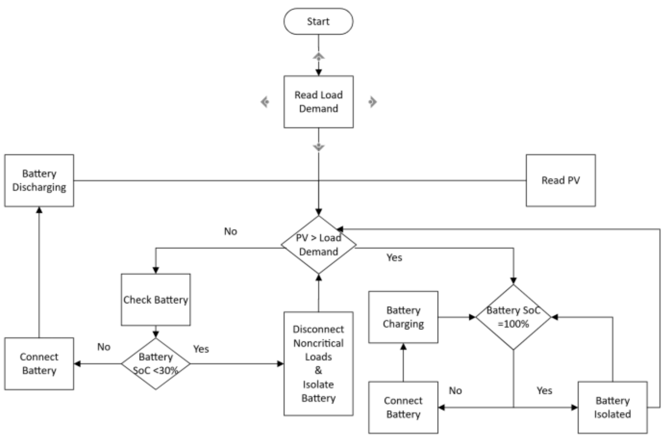

Fig. 8: Prototype control logic flowchart
Source: created by the authors.

Table 2. Prototype main components and costs

Component	Power	Voltage	Current	Cost
Solar panel	255 W	30.8 Vmp	8.28 A	$145.46
Battery	640Wh	12.8 VDC	50Ah	$99.99
Inverter	400W–800W	24VDC – 110VAC	3A Max	$38.68
Charge controller		12–24 VDC	10 A	$9.99
Buck Converter		Input: 6V DC – 32V DC Output: 1.5V DC – 32V DC	5A Max	$16.99
Total				**$311.11**

Note: Cost of small components such as resistors is not included.
Source: created by the authors.

In Figure 11, the prototype is fully operational. The red LEDs in this setup are all off, indicating that power is being supplied to all AC and DC loads (i.e., both non-critical and critical loads). We can see that the display shows the battery being charged at 13.4V and its SOC is at 90%. At this stage, all relay control pins are set to HIGH, effectively disabling all the relays from blocking power to the loads. In this context, "disabling" the relays means they no longer block current, so all connected loads are powered on. All red LEDs on the relay module turn off, indicating that each relay now allows power to go through. This mode signifies that the battery has sufficient energy to safely operate the entire system (i.e., supplying power to all loads).

In Figure 12, we can see on the LCD display showing the battery voltage of 13.1V and SOC of 40%. At this state only critical loads are on which are indicated by their relays whose red LEDs are off. Furthermore, the noncritical loads have no power supply which is indicated by their respective red LEDs being on. As the battery charges and the voltage reaches between 12.9V and 13.2V, the system transitions into a partial activation mode. In this state, only essential loads are powered. Specifically, the control pins for RELAY_CHARGING and RELAY_DC_CRIT are set to HIGH (relays disabled), while RELAY_AC and RELAY_DC_NONCRIT are set to LOW (relays enabled). Due to the inverted control logic, this means that only the critical DC loads and the battery charging circuit are allowed to operate, while non-critical loads such as AC or auxiliary DC loads remain disabled. This selective activation helps reduce strain on the battery while still maintaining essential operations. Overall, the test results show that the prototype works properly. The microcontroller automatically controls the load relays to turn on and turn off the loads appropriately based on the battery power availability.

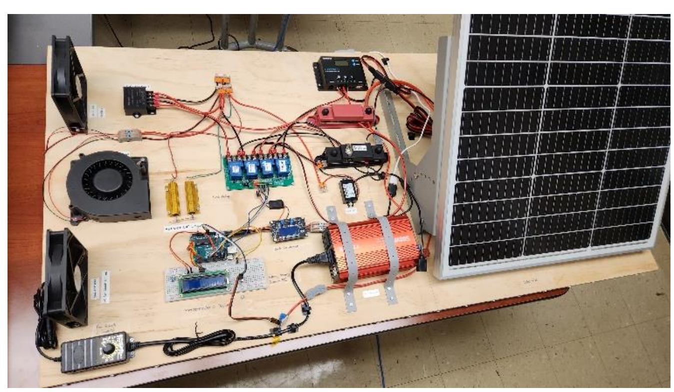

Fig. 9: Completed prototype; the battery is located behind the solar PV panel on the right side
Source: created by the authors.

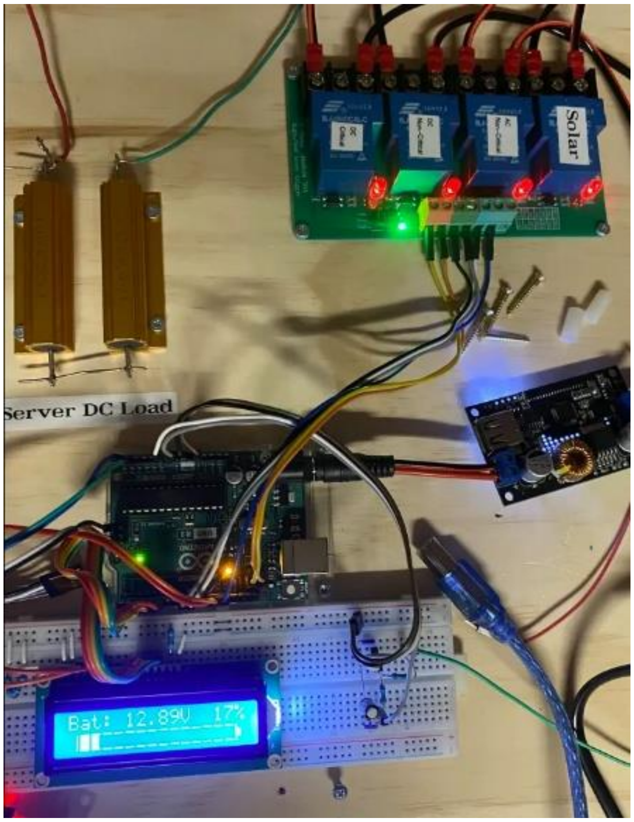

Fig. 10: The system is turned on; no power is distributed to loads because the battery SOC is below 30%

Source: created by the authors.

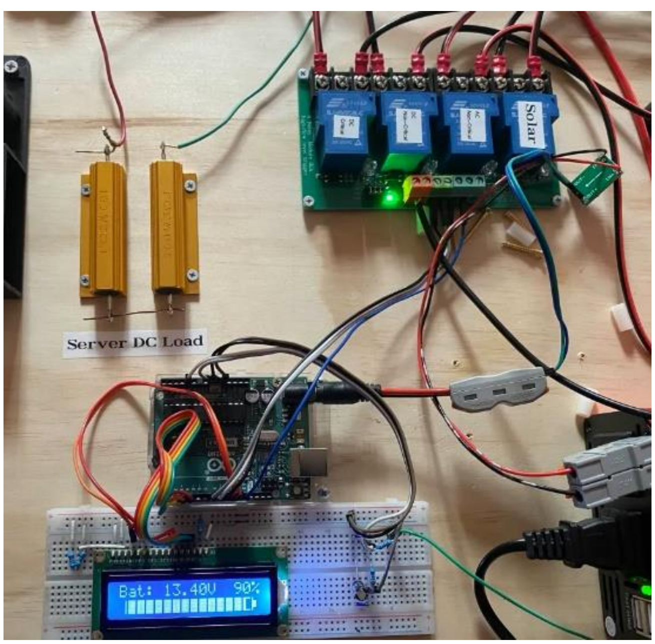

Fig. 11: The system is fully operational and provides power to all loads; battery SOC is 90%

Source: created by the authors.

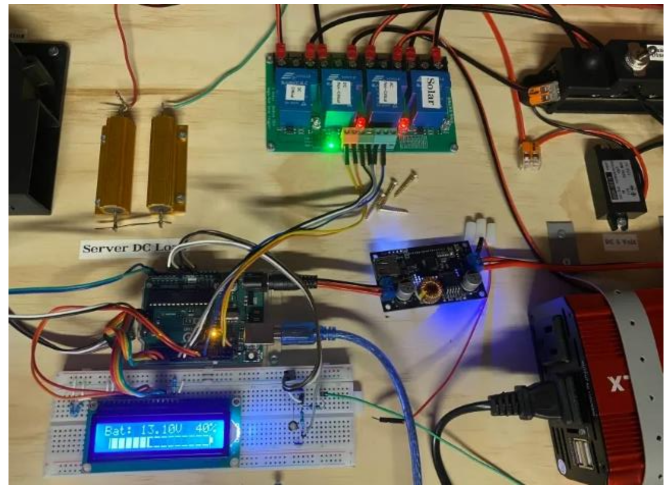

Fig. 12: The battery feeds critical loads; non-critical loads are turned off; battery SOC is 40%

Source: created by the authors.

5 Lessons Learned

One of the main takeaways experienced with the voltage sensing based on Arduino implementation, was an understanding of the importance of having a common ground bond connecting the Arduino to the voltage source when measuring the voltage of an outside power supply with an Arduino. The Arduino's analog-to-digital converter (ADC) is measuring the input voltage to it with reference to its own ground reference. If we do not have a common ground bond, we do not have a proper reference voltage, and we lose our measurement relevance, which in this case means a lot of floating and non-sensible readings which can have an impact on the integrity of the measurement.

We added value with the capacitive filtering as the initial implementation voltage sensed accuracy was significantly improved. When capacitors work properly, they do a good job smoothing voltage sensing, being able to effectively filter-out rapid fluctuations and ripples that can occur with the voltage signal. The capacitor stores physical electric charge when the voltage rises, and then through discharging it when the voltage drops. This way, it has the ability to maintain a more constant voltage level at the measurement location. This process ultimately serves to improve sensing reliability and sensing stability.

To solve the battery SOC sensing issues, we focused on improving the accuracy of battery voltage measurement and accurately mapping the sensed voltage to the battery's SOC using a standardized discharge curve. The first step involved adding a 100µF capacitor across the microcontroller analog input and ground. This capacitor helps smooth out high-frequency noise and voltage ripples, resulting in a cleaner signal for analog-to-digital conversion. The second step was to improve voltage sensing precision by implementing a voltage divider using well-matched resistors (R1 = 30kΩ and R2 = 7.5kΩ), which safely scaled the battery voltage down to a range suitable for the Arduino's 10-bit ADC.

Despite these hardware improvements, minor fluctuations persisted due to ADC noise and environmental interference. To address this issue, we used a software-based averaging method to further stabilize the measurement reading. The function below shows how we took multiple ADC samples, averaged them, and then applied the voltage divider ratio to calculate the actual battery voltage:

```
float readVoltage() {
  const int samples = 10;
  long sum = 0;
  for (int i = 0; i < samples; i++) {
    sum += analogRead(ANALOG_INPUT);
    delay(5);
  }
  float avg = sum / float(samples);
  float vout = avg * 0.00494125; // 5V / 1024 for 10-bit
ADC
  return vout / (R2 / (R1 + R2));
```

The ADC scale factor (originally 5.0 / 1024) was slightly adjusted based on calibration against a digital multimeter. This fine-tuning ensured that the voltage reported by the Arduino matched closely with actual battery voltage, improving overall SOC accuracy.

By averaging multiple readings, we were able to reduce short-term fluctuations and achieve a more stable and accurate voltage measurement. To further enhance reliability, especially for relay control, we applied a small software voltage offset of approximately +0.05V. This compensates for ADC reference inaccuracies, battery rebound effects, and small voltage drops in wiring. Without this adjustment, the relay module was prone to flickering, as minor voltage shifts would rapidly toggle its state near the switching threshold.

6 Conclusion

In this project, we successfully designed and implemented a microgrid for enhancing the reliability of power supply to a 5.85-MW AI data center. The realistic microgrid is designed to meet 60% of the data center energy demand while the remaining 40% is provided by the utility grid. The microgrid has a solar PV and a battery system that provide power to the center load during daytime and nighttime. The solar PV system size is 13600kW which sufficiently supports 60% of the center load demand while charging the battery during daytime. The battery can power the center load at night for up to 18.2 hours. Under grid outages, the solar PV and battery systems can continue to provide power to the center, thereby helping increase its reliability and avoid interruption of critical services.

The microgrid design concepts and performance is evaluated by building a prototype that resembles it. Testing results show that the prototype works properly, which suggests that the design concepts are valid. The power supply to the prototype critical and non-critical loads are managed automatically and effectively by a control system which includes a microcontroller, sensors and relays.

The project demonstrates that a hybrid renewable system is sustainable and can effectively meet the growing demand of data centers. The microgrid concepts are applicable to all AI data centers where space and resource are available for solar PV. Its outcomes show the scalable model to enhance power supply reliability for AI data centers and their service continuity while lowering carbon emissions and reducing power demand stress on utility grids.

References:

[1] M. Uddin, H. Mo, D. Dong, S. Elsawah, J. Zhu, and J. M. Guerrero, "Microgrids: A review, outstanding issues and future trends," *Energy Strategy Reviews,* vol. 49, p. 101127, 2023.

[2] K. Kant, "Data center evolution: A tutorial on state of the art, issues, and challenges," *Computer Networks,* vol. 53, no. 17, pp. 2939-2965, 2009.

[3] E. Oró, V. Depoorter, A. Garcia, and J. Salom, "Energy efficiency and renewable energy integration in data centres: Strategies and modelling review," *Renewable and Sustainable Energy Reviews,* vol. 42, pp. 429- 445, 2015.

[4] A. Orr, K. Gentle, and E. Hesla, "Utility services for data centers," presented at the 2020 IEEE/IAS 56th Industrial and Commercial

Power Systems Technical Conference (I&CPS), 2020.

[5] T. I. Vasques, P. Moura, and A. de Almeida, "A review on energy efficiency and demand response with focus on small and medium data centers," *Energy Efficiency,* vol. 12, pp. 1399-1428, 2019.

[6] L. Bajracharyay, S. Awasthi, S. Chalise, T. M. Hansen, and R. Tonkoski, "Economic analysis of a data center virtual power plant participating in demand response," presented at the 2016 IEEE Power and Energy Society General Meeting (PESGM), 2016.

[7] M. Ghamkhari and H. Mohsenian-Rad, "Optimal integration of renewable energy resources in data centers with behind-the- meter renewable generator," presented at the 2012 IEEE international conference on communications (ICC), 2012.

[8] M. H. Rehmani, M. Reisslein, A. Rachedi, M. Erol-Kantarci, and M. Radenkovic, "Integrating renewable energy resources into the smart grid: Recent developments in information and communication technologies," *IEEE Transactions on Industrial Informatics,* vol. 14, no. 7, pp. 2814-2825, 2018.

[9] M. Haddad, "Sizing and management of hybrid renewable energy system for data center supply," Université Bourgogne Franche-Comté, 2019.

[10] C. Guo, F. Luo, Z. Cai, and Z. Y. Dong, "Integrated energy systems of data centers and smart grids: State-of-the-art and future opportunities," *Applied Energy,* vol. 301, p. 117444, 2021.

[11] C. C. Thompson, P. K. Oikonomou, A. H. Etemadi, and V. J. Sorger, "Optimization of data center battery storage investments for microgrid cost savings, emissions reduction, and reliability enhancement," *IEEE Transactions on Industry Applications,* vol. 52, no. 3, pp. 2053-2060, 2016.

[12] D. Wang, C. Ren, A. Sivasubramaniam, B. Urgaonkar, and H. Fathy, "Energy storage in datacenters: what, where, and how much?," presented at the Proceedings of the 12th ACM SIGMETRICS/PERFORMANCE joint international conference on Measurement and Modeling of Computer Systems, 2012.

[13] O. Aguilar, R. Ceballos, M. A. Garcia, M. E. Hernandez, D. T. Hoang, J. Rodela, B. Sysavath, L. Villanueva, and H. T. Le, "Stand-alone Hybrid Solar-Wind Microgrid for Providing Clean and Reliable Energy to Disadvantaged Communities," *WSEAS Transactions on Power Systems,* vol. 20, no. Article 12, pp. 133-162, 2025, doi: 10.37394/232016.2025.20.12.

[14] K. J. Vallejos, E. Fernandez, A. Larkin, D. Cabrera, O. R. Diaz, A. Valle, A. Vu, T. Yim, O. Aljumaa, O. Sierra, M. Alcala, N. Garcia, T. Bailey, S. Yau, and H. T. Le, "Enhancing Power Balancing and Fault Interruption in an Autonomous Smart Microgrid Design," *International Journal of Power Systems,* vol. 7, pp. 42-67, 2022.

[15] H. N. Ho, T. Bui, H. Do, E. Rojas, O. Ojeda, H. Tran, T. Hoang, E. Hernandez, L. Nguyen, and H. T. Le, "Design and Simulation of an Autonomous Smart Microgrid for Energy Independence," *WSEAS Transactions on Environment and Development,* vol. 17, pp. 911-928, 2021, doi: 10.37394/232015.2021.17.85

[16] S. Chen, C. Gonzalez, C. Diaz, K. Leung, A. Liu, N. Lopez, N. Nguyen, A. Phung, A. Uzueta, K. Wooden, and H. T. Le, "A Mobile Green Power Source for Emergency and Special Purposes Using Solar and Wind Power," *WSEAS Transactions on Circuits and Systems,* vol. 20, pp. 215-226, 2021, doi: 10.37394/23201.2021.20.25.

[17] A. El Khaouat and L. Benhlima, "Distributed integrated control system architecture for microgrids," presented at the 2018 19th IEEE Mediterranean Electrotechnical Conference (MELECON), 2018. https://doi.org/10.1109/MELCON.2018.8379059.

[18] A. Scarfò, "The evolution of data center networking technologies," presented at the 2011 First International Conference on Data Compression, Communications and Processing, 2011. https://doi.org/10.1109/CCP.2011.30.

[19] G. Ghatikar, M. A. Piette, S. Fujita, A. McKane, J. H. Dudley, A. Radspieler, K. C. Mares, and D. Shroyer, "Demand Response and Open Automated Demand Response Opportunities for Data Centers," Lawrence Berkeley National Laboratory, 2010, [Online]. https://eta-publications.lbl.gov/sites/default/files/demand_response_and_open_automated_demand_respons

e_opportunities_for_data_centers_lbnl-3047e.pdf (Accessed Date: January 10, 2026).

[20] National Renewable Energy Laboratory PVWatts calculator, [Online]. https://pvwatts.nrel.gov/pvwatts.php (Accessed Date: January 10, 2026).

[21] Monocrystalline, "50W Solar Panel," 2025, [Online]. https://www.etrailer.com/dept-pg-RV_Solar_Panels.aspx https://www.etrailer.com/dept-pg-RV_Solar_Panels.aspx (Accessed Date: January 10, 2026).

[22] Bawaut, "Inverter" 2025, [Online]. https://bawaut.com/products/500w-power-inverter-dc-12v-to-ac-converter https://bawaut.com/products/500w-power-inverter-dc-12v-to-ac-converter (Accessed Date: January 10, 2026).

[23] "12V 50Ah LiFePO4 Deep Cycle Battery,4000+ Cycles Lithium Iron Phosphate Rechargeable Battery for Solar".

[24] Naz, "Charge Controller," 2025, [Onine]. https://www.solar-electric.com/search/?q=Charge+Controller (Accessed Date: January 10, 2026).

[25] Drok, "Buck Converter," 2025, [Online]. https://www.droking.com/Adjustable-Buck-Boost-Converter-Board-DC-5.5-30V-to-0.5-30V-4A-High-Power-Supply-Regulator-with-Case-LCD-Display (Accessed Date: January 10, 2026).

[26] LiFePO4, "Battery," 2025, [Online]. https://www.renogy.com/deep-cycle-batteries/ (Accessed Date: January 10, 2026).

Contribution of Individual Authors to the Creation of a Scientific Article (Ghostwriting Policy)

Ramon Zintzun, Ethan Hoang, Jared Wong, Akanksha Katta, Vinh Nguyen, Alex Villaneda, Gerardo Maximo: background literature review, design of theoretical microgrid, design, implementation and testing of prototype, writing first draft of paper. Ha Thu Le: refining research issues and scope, methodology, technical advising, solar PV system sizing, review of results, formatting and editing final draft, revising reviewed paper to meet reviewer requirements.

Sources of Funding for Research Presented in a Scientific Article or Scientific Article Itself

No funding was received for conducting this study.

Conflict of Interest

The authors have no conflicts of interest to declare that are relevant to the content of this article.

Declaration of Generative AI and AI-assisted Technologies in the Writing Process

The authors declare that no AI-assisted technologies have been used in writing this paper.

APPENDIX

Table 3. Battery discharge curve used for sensing its state of charge (SOC)

Voltage	Capacity
14.4V	100%
13.6V	100%
13.4V	99%
13.3V	90%
13.2V	70%
13.1V	40%
13.0V	30%
12.9V	20%
12.8V	17%
12.5V	14%
12.0V	9%
10.0V	0%

Source: [26]

Microcontroller code:

```
 #include <LiquidCrystal.h>

// LCD pins: RS, E, D4, D5, D6, D7
const int rs = 12, en = 11, d4 = 5, d5 = 4, d6 = 3, d7 = 2;
LiquidCrystal lcd(rs, en, d4, d5, d6, d7);

// Analog input pin
const int analogInput = A1;

// Voltage divider resistors
const float R1 = 30000.0;
const float R2 = 7500.0;

// Relay control pins
#define RELAY_CHARGING     13
#define RELAY_DC_CRIT      10
#define RELAY_AC           9
#define RELAY_DC_NONCRIT    8

// Battery gauge characters
byte gauge_empty[8]  = [1 B00000, B00000, B00000, B00000,
      B11111, 2];
byte gauge_fill_1[8] = [3 B10000, B10000, B10000, B10000,
      B11111];
byte gauge_fill_2[8] = [4 B11000, B11000, B11000, B11000,
      B11111];
byte gauge_fill_3[8] = [7 B11100, B11100, B11100, B11100,
      B11111];
byte gauge_fill_4[8] = [7 B11110, B11110, B11110, B11110,
      B11111];
byte gauge_fill_5[8] = [10 B11111, B11111, B11111, B11111,
      B11111];
byte gauge_mask_left[8] = [5 B00001, B00001, B00001, B00001,
      B00001];
byte gauge_mask_right[8] = [6 B11100, B11100, B11100,
      B10000, B10000];

byte gauge_left_dynamic[8], gauge_right_dynamic[8];
char gauge_string[17]; // 16 + null terminator
char buffer[17];

float vin = 0.0;
int battery_percent = 0;
const int gauge_size_chars = 16;

void setup() {
  pinMode(RELAY_CHARGING, OUTPUT);
  pinMode(RELAY_DC_CRIT, OUTPUT);
  pinMode(RELAY_AC, OUTPUT);
  pinMode(RELAY_DC_NONCRIT, OUTPUT);

  pinMode(analogInput, INPUT);
  lcd.begin(16, 2);
  Serial.begin(9600);

  // Create static gauge fill levels
  lcd.createChar(7, gauge_empty);
  lcd.createChar(1, gauge_fill_1);
  lcd.createChar(2, gauge_fill_2);
  lcd.createChar(3, gauge_fill_3);
  lcd.createChar(4, gauge_fill_4);

  lcd.clear();
  lcd.setCursor(0, 0);
  lcd.print("LOADING...");
  delay(3000);
}

void loop() {
  vin = readVoltage();
  battery_percent = voltageToPercent(vin);
  controlRelays(vin);
  updateBatteryGauge();
  delay(300);
}

float readVoltage() {
  int input = analogRead(analogInput);
  float vout = input *  0.0048890325; // 5 / 1024
  return vout / (R2 / (R1 + R2));   // Reverse divider calc
}

void controlRelays(float voltage) {
   const float buffer = 0.05; // 50mV buffer zone to avoid
      flickering
  if (voltage < 12.88) {
    // ALL OFF
    digitalWrite(RELAY_CHARGING, HIGH);
    digitalWrite(RELAY_DC_CRIT, HIGH);
    digitalWrite(RELAY_AC, HIGH);
```

```
    digitalWrite(RELAY_DC_NONCRIT, HIGH);

  }
  else if (voltage > 12.94 && voltage < 13.18) {
    // CHARGING + DC CRITICAL only
    digitalWrite(RELAY_CHARGING, LOW);
    digitalWrite(RELAY_DC_CRIT, LOW);
    digitalWrite(RELAY_AC, HIGH);
    digitalWrite(RELAY_DC_NONCRIT, HIGH);
  }
  else if (voltage > 13.5) {
    // ALL ON
   digitalWrite(RELAY_CHARGING, LOW);
    digitalWrite(RELAY_DC_CRIT, LOW);
    digitalWrite(RELAY_AC, LOW);
    digitalWrite(RELAY_DC_NONCRIT, LOW);
  }
}

int voltageToPercent(float voltage) {
  if (voltage >= 14.6) return 100;
  if (voltage >= 13.6) return 100;
  if (voltage >= 13.4) return 99;
  if (voltage >= 13.3) return 90;
  if (voltage >= 13.25) return 70;

  if (voltage >= 13.1) return 40;
  if (voltage >= 13.0) return 30;
  if (voltage >= 12.9) return 20;
  if (voltage >= 12.8) return 17;
  if (voltage >= 12.5) return 14;
  if (voltage >= 12.0) return 10;
  if (voltage >= 10.0) return 0;

  return 0;
}

void updateBatteryGauge() {
  int value_in_pixels = round(battery_percent * (gauge_size_chars
      * 5.0) / 100.0);
  int move_offset = 4 - ((value_in_pixels - 1) % 5);

  for (int i = 0; i < 8; i++) {
    gauge_left_dynamic[i] = gauge_fill_5[i] & gauge_mask_left[i];
    gauge_right_dynamic[i] = gauge_fill_5[i] &
      gauge_mask_right[i];
  }

  lcd.createChar(5, gauge_left_dynamic);
  lcd.createChar(6, gauge_right_dynamic);

  for (int i = 0; i < gauge_size_chars; i++) {
    if (i == 0)
      gauge_string[i] = byte(5);
    else if (i == gauge_size_chars - 1)
      gauge_string[i] = byte(6);
    else if (value_in_pixels <= i * 5)
      gauge_string[i] = byte(7);
    else if (value_in_pixels < (i + 1) * 5)

      gauge_string[i] = byte(5 - move_offset);
    else
      gauge_string[i] = byte(255);
  }

  char voltageStr[8];
  dtostrf(vin, 5, 2, voltageStr);  // Format voltage to string

  lcd.setCursor(0, 0);
  sprintf(buffer, "Bat: %sV %3d%%", voltageStr, battery_percent);
  lcd.print(buffer);
  lcd.setCursor(0, 1);
  lcd.print(gauge_string);

  Serial.print("Vin: "); Serial.print(vin, 2); Serial.print(" V, ");
  Serial.print("Battery: "); Serial.print(battery_percent);
      Serial.println(" %");
}
```